Pergamon

*Journal of Structural Geology*, Vol. 16, No. 6, pp. 823 to 838, 1994

0191-8141/94 $07.00+0.00

# Re-evaluation of extension across the Pearl River Mouth Basin, South China Sea: implications for continental lithosphere deformation mechanisms

ROB WESTAWAY

16 Neville Square, Durham DH1 3PY, U.K.

(*Received* 15 *September* 1992; *accepted in revised form* 8 *August* 1993)

**Abstract**—The Tertiary Pearl River Mouth Basin in the South China Sea is one of relatively few localities where independent estimates of extension from upper-crustal normal faulting, crustal thinning and subsidence have been compared. Previous work indicates that these methods all support extension factor $\beta = 1.8$ for this basin. However, the estimate from faulting used the controversial rigid domino method, whereas summing normal fault heaves gives $\beta$ only 1.3 instead. This study pursues the possibility that the true $\beta$ value for this basin is 1.3, and the published estimates of extension from subsidence and crustal thinning are exaggerated because they do not take account of outflow of lower-crustal material from beneath this basin. Such outward channel flow will occur when the lithostatic pressure at the base of the brittle upper crust is greater beneath a basin than beneath its surroundings. In response to such a pressure gradient, material lost from beneath this basin has probably flowed to beneath the adjacent Chinese landmass, where it isostatically compensates the erosion that has supplied much of the basin's sediment.

## INTRODUCTION

RECENT developments in theory and observation have stimulated new ideas concerning the principles governing extension of the continental lithosphere. First, a growing body of evidence indicates that deformation of basement in the surroundings to planar normal faults that cut the brittle upper crust can be regarded as distributed vertical simple shear (e.g. Wernicke *et al.* 1988, Axen & Wernicke 1991, Westaway 1992a, 1993, Westaway & Kusznir 1993). This means that the extension across any planar normal fault equals its heave. Analysis of extension can thus be simplified compared with other structural methods, because the extension across any region equals the sum of heaves of normal faults within it.

Second, it has been suggested that channel flow can occur in the lower crust, which is weak compared with its surroundings (above and below) and can be regarded as a fluid on long time scales (e.g. Wernicke 1990, Kruse *et al.* 1991). Channel flow means flow parallel to planar boundaries, in this case between the base of the brittle upper crust and the Moho. Horizontal flow to maintain isostatic equilibrium may in principle occur instead in the asthenosphere. However, because its viscosity, which is no less than $\sim 10^{20}$ Pa s (e.g. Peltier 1982), exceeds that of the lower crust (no greater than $\sim 10^{19}$ Pa s—see Appendix 3), flow in the lower crust is more likely to be important.

Kruse *et al.* (1991) investigated Tertiary extension of the Basin and Range province (BRP) in the western U.S.A. They deduced that lower crustal flow was inward, to beneath this extensional province. As a result of the geometry of river systems, BRP extension has been accompanied by minimal influx of sediment from its surroundings. Its arid climate also restricts local erosion, such that many of its normal-fault-bounded basins do not contain much sediment. These conditions are atypical of many other extensional provinces. With more rapid sedimentation and/or erosion of the surroundings of an extensional province, lower-crustal flow may instead be outward. Loss of lower-crustal material has indeed been suggested as a qualitative explanation for 'extension discrepancies', between estimates of extension from faulting and crustal thinning (e.g. Ziegler 1983). New theory, to quantify this flow and its effects and to address the conditions for it to be inward or outward, is presented in Appendices 1–4.

It has been accepted (e.g. McKenzie 1978), and incorporated into standard procedures for modelling extensional basins, that the isostatic response to crustal extension (and associated processes such as sediment loading and erosion) occurs by vertical deflection of the Moho, not horizontal flow in the lower crust. Faulting in the brittle upper crust is also often represented using empirical schemes such as 'rigid dominoes' (e.g. Jackson & McKenzie 1983). It is important to assess the implications of the views that extension of the upper crust is associated with vertical shear, and its isostatic compensation involves lower-crustal flow. They may, for instance, allow existing observations of basins to be consistent with values of extension factor $\beta$ that differ from predictions using traditional methods (e.g. Westaway & Kusznir 1993).

To test whether modelling incorporating vertical shear in the upper crust and channel flow in the lower crust can match observations of basins in terms of different amounts of extension from other methods, it is necessary to identify a suitable case study locality. The Pearl River Mouth Basin (PRMB) in the South China Sea (Fig. 1) is selected for four main reasons. First, high-quality data constrain key observations such as positions

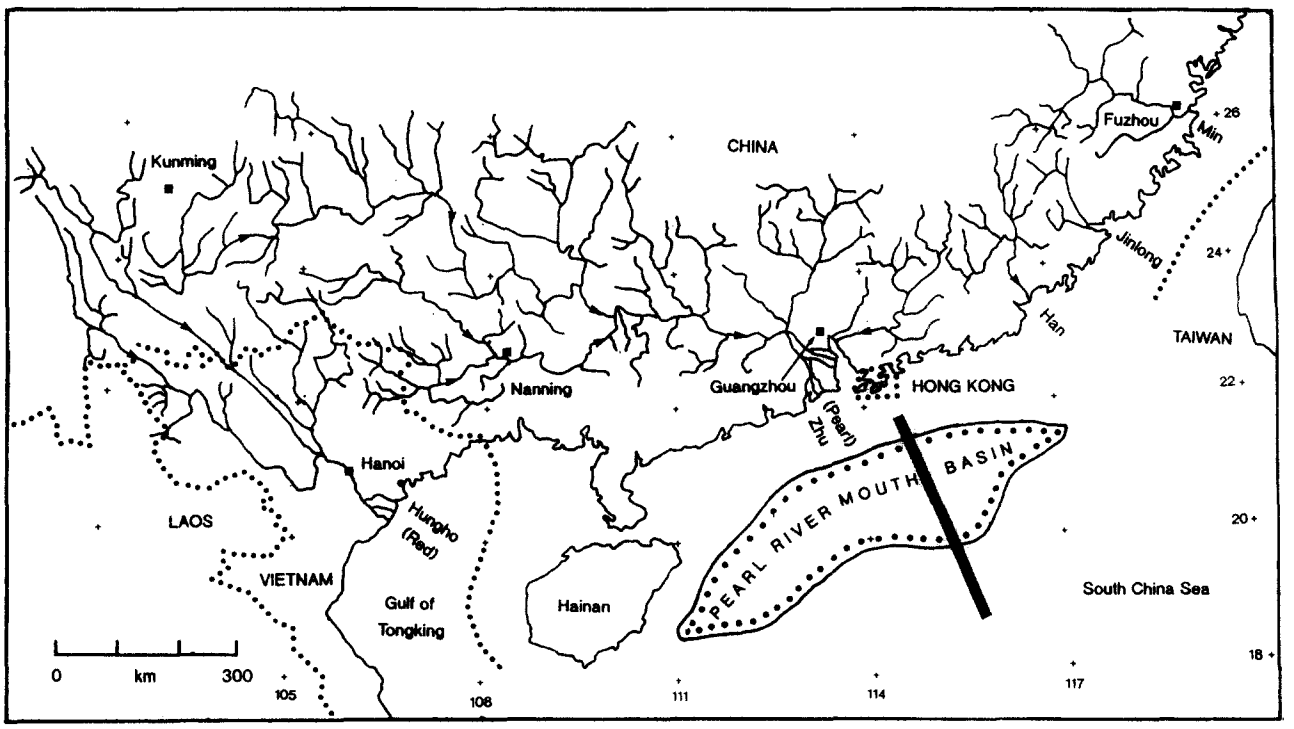


Fig. 1. Regional map showing the Pearl River Mouth Basin within the South China Sea, and river systems in the eroding Chinese landmass. Position of the profile in Fig. 2 is also shown. The Red River fault zone is highlighted by the southeast trend of the Red River and its tributaries.

of formation boundaries and faults, and allow precise estimates of the derived parameter $\beta$ to be made, subject to the assumption of particular analysis methods. The result that different methods give different $\beta$ values for this basin is thus not caused by uncertain or inadequate data. Second, the overall geometry of this basin, for deposition and sediment supply, is clear. Third, local conditions (low initial elevation, low extensional strain, rapid sedimentation, and sediment source within a few hundred kilometres) favour substantial outward lower-crustal flow. Finally, this locality has not previously been used to develop structural models, and thus provides an independent test for models established elsewhere.

This article thus has the following objectives. First, the PRMB is described, and the extension across it is re-evaluated by summing the heaves of its normal faults. This gives a much lower estimate for $\beta$ than has been suggested previously. Second, application of new quantitative theory, which incorporates loss of lower-crustal material by outward channel flow, is shown also to account for the form of this basin in terms of this low value of $\beta$. Finally, tests for this theory, and its general implications, are discussed.

## THE PEARL RIVER MOUTH BASIN: OBSERVATIONS

The Pearl River Mouth or Zhujiangkou Basin (PRMB) is in the South China Sea, offshore of Hong Kong and southern China (Fig. 1). It is 800 km long in the WSW–ENE direction, up to 300 km wide, and has taken up Tertiary extension on many normal faults (see e.g. Feng *et al.* 1992 or Edwards 1992 for detailed fault maps). Some localities show complex faulting, with many adjacent normal faults. Elsewhere, major normal faults are up to ~80 km apart (Fig. 2). The Tertiary stratigraphy of the PRMB (Table 1) indicates fluvial and lacustrine sedimentation (the Shenhu, Wenchang and Enping formations) before Oligocene time (i.e. before ~40 Ma), various coastal environments (the Zhuhai, Zhujiang and Hanjiang formations) during Oligocene to Middle Miocene time (i.e. ~40–10 Ma), and shallow marine conditions (the Yehai and Wanshan formations) since, and thus suggests overall subsidence relative to sea level.

### *Timing of extension*

Although it is clear that most—if not all—PRMB extension occurred during early Tertiary time, its precise timing has been controversial. From analysis of subsidence, Ru & Pigott (1986) suggested three phases of extension, during late Cretaceous to middle Paleocene (~70–60 Ma; $\beta$ = 1.2), late Eocene to middle Oligocene (~40–30 Ma; $\beta$ = 1.7), and middle Miocene (~15–10 Ma; $\beta$ = 1.6), making the overall extension factor ~3.1. However, they calculated thermal subsidence following each phase assuming instantaneous extension. Su *et al.* (1989) noted that this overestimates $\beta$ compared with calculations for finite durations of extension. They suggested instead that most extension ($\beta$ ~1.8) occurred during 60–35 Ma, with some ($\beta$ ~1.1) during 25–11 Ma. Wang *et al.* (1992) also suggested two phases of extension, but during ~70–63 Ma and 32–17 Ma. Feng *et al.* (1992) suggested a single phase during middle Oligocene to early Miocene time, or ~30–15 Ma.

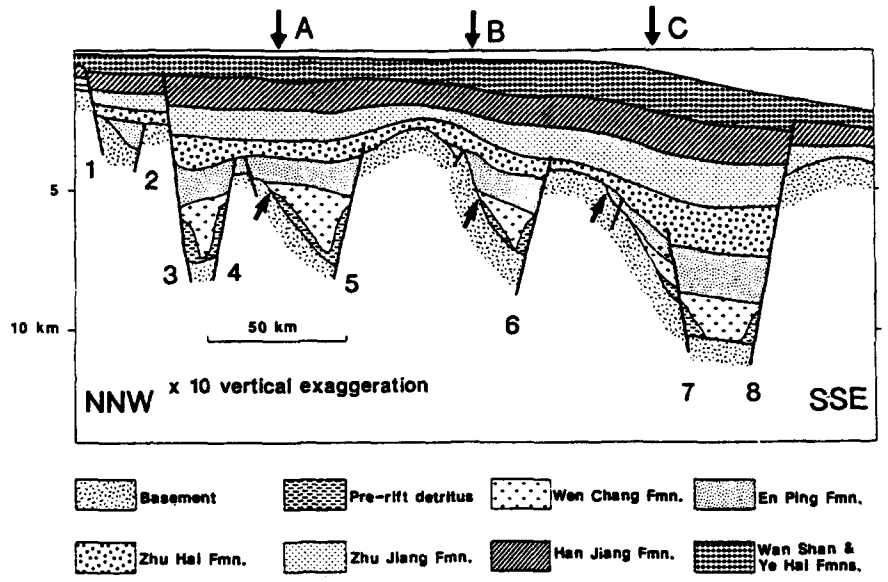


Fig. 2. Cross-sectional profile along the line shown in Fig. 1, adapted from fig 5(c) of Su *et al.* (1989). Formations are described in Table 1. Top Enping Formation marks the end of the main phase of extension, according to Su *et al.* (1989). Downward arrows labelled A, B and C indicate the three blocks used in the rigid domino analysis by Su *et al.* (1989). Diagonal arrows point to example localities in these blocks where the local tilt equals the amount used in their analysis. Numbers indicate normal faults whose heaves give the extension along this profile in the analysis in this study.

Edwards (1992) also suggested a single phase of extension, during 36–26 Ma.

PRMB extension thus occurred during deposition of the upper Shenhu, Wenchang and Enping formations according to Su *et al.* (1989), or during deposition of the Enping and Zhuhai formations according to Edwards (1992). The different stratigraphic chronologies (Table 1) cause additional complication in dating PRMB extension. The 60–35 Ma main phase of extension suggested by Su *et al.* (1989) adjusts to 45–30 Ma with the Edwards (1992) chronology. The 35–26 Ma timing deduced by Edwards (1992) adjusts to 43–23 Ma if the Chen & Li (1987) chronology (used by Su *et al.* 1989) is used instead.

According to Su *et al.* (1989) the main constraint on the end of the early Tertiary phase of PRMB extension is that the Zhuhai and younger formations are not cut by most normal faults (Fig. 2). Their minor offsets across some faults (noted, for example, by Edwards 1992) can be attributed to greater compaction of the thicker sedimentary sequences on the hanging-wall sides. Following this interpretation, the Enping and older formations can be regarded as 'syn-rift', and the Zhuhai and younger formations as 'post-rift'. Thickness of syn-rift sediment in the PRMB thus ranges from 0 to 3 km, averaging ~1.5 km. Thickness of post-rift sediment ranges from 2 to 6 km, averaging ~3.5 km. Overall sediment thickness ranges from 2 to 9 km, averaging ~5 km. This ~5 km typical sedimentation (Fig. 2) in ~60 Ma indicates time-averaged sedimentation rate ~0.08 mm year$^{-1}$. The ~3.5 km typical post-Enping thickness indicates rate ~0.1 mm year$^{-1}$ since ~35 Ma. The ~1 km thickness of the Wanshan and Yehai formations (age ~11–2 Ma) indicates rate ~0.11 mm year$^{-1}$ for this most recent time scale.

The main evidence for the second phase of extension suggested by Su *et al.* (1989) is the rapid subsidence during deposition of the middle Miocene Hanjiang formation, which is typically ~1 km thick (Fig. 2). Their chronology dates its duration as only ~3 Ma, requiring sedimentation rate ~0.3 mm year$^{-1}$—much higher than the above values at other times. However, with the 7 Ma duration preferred by Edwards (1992), sedimentation rate 0.14 mm year$^{-1}$ is deduced instead, similar to these values.

Investigations by Tapponnier *et al.* (1990) indicate the likely cause of extension in the PRMB and neighbouring basins. They studied the Red River fault zone, a >1000 km long SE-trending strike-slip fault zone in southern China and northern Vietnam. They showed this took up ~500 km of left-lateral slip between ~60–50 Ma and ~15–20 Ma, indicating time-averaged slip rate ~10–15 mm year$^{-1}$. This fault zone accommodated southeastward displacement of Indochina relative to Eurasia during early stages of the collision between India and Eurasia (Fig. 3). North–south – northwest–southeast sea-floor spreading occurred in the central South China Sea during ~32–17 Ma (Taylor & Hayes 1982), creating up to 700 km width of oceanic lithosphere. The southern margin of the PRMB is within ~100 km of the northern edge of this oceanic lithosphere, which at present has ~3–4 km bathymetry. As drawn in Fig. 3, the Red River fault has typical concave-southward radius of curvature ~1200 km. Left-lateral slip on it thus requires clockwise rotation of Indochina relative to southern China. The recent discovery, using palaeomagnetism, of ~25° of rotation in this sense (Funahara *et al.* 1993) is consistent with ~500 km left-lateral displacement on the Red River fault (~500 km arc length divided by ~1200 km radius of curvature is ~0.42 radian, roughly 25°). The Red River fault zone at present accommodates right-lateral slip instead, at ~2–5 mm year$^{-1}$ (Allen *et al.* 1984). Its ~5.5

km right-lateral offset indicates that slip in this sense began at ~3–1 Ma, long after the earlier left-lateral slip ceased.

Extension in the PRMB and neighbouring basins and later sea-floor spreading in the South China Sea most likely occurred to take up southeastward or SSE relative motion of Eurasia and Indochina, consistent with left-lateral slip on the Red River fault. Figure 3 summarizes three stages of this process: at ~50 Ma shortly after this fault became active, with extension occurring in a broad zone across much of the South China Sea; at ~30 Ma during the early stages of sea-floor spreading; and at ~20 Ma shortly before this spreading ceased. A similar left-lateral fault zone in Thailand and the Gulf of Thailand accommodated southeastward relative motion between Malaya and Indochina at around the same time, which was taken up farther east by extension in the southwestern part of the South China Sea (Tapponnier *et al.* 1990).

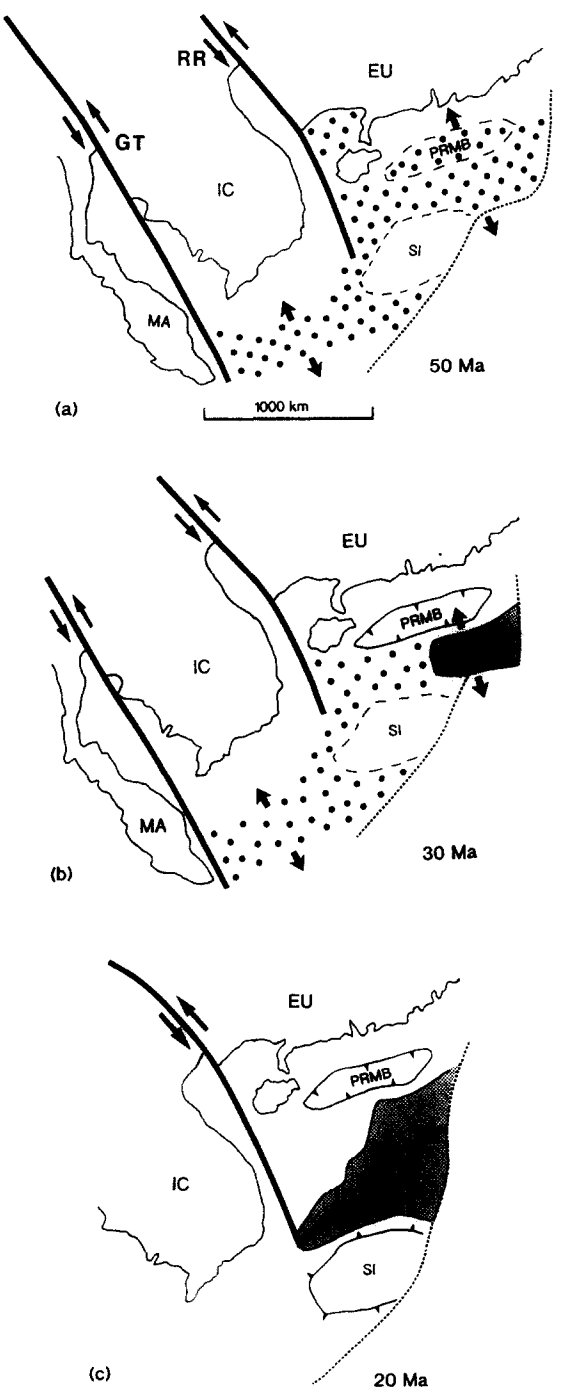


The 60 Ma start of PRMB extension suggested by Su *et al.* (1989) roughly matches the start of slip on the Red River fault. Their ~35 Ma end of PRMB extension roughly matches the start of sea-floor spreading in the central South China Sea. Once this spreading began, it could readily accommodate all relative motion of Indochina and Eurasia, with no need for a broad zone of distributed extension. These considerations support the ~60–35 Ma timing or PRMB extension suggested by Su *et al.* (1989). They are also roughly consistent with the ~45–30 Ma timing that results from using the Su *et al.* (1989) interpretation of PRMB structure and the Edwards (1992) chronology. However, any extension significantly later would require a different cause.

Rapidly-extending regions, such as the Aegean (e.g. Jackson & McKenzie 1988), extend at strain rate $\sim 10^{-15}$ $s^{-1}$. The extensional strain (equal to $\beta - 1$) across a region can be estimated as its strain rate multiplied by the duration of extension. At strain rate $10^{-15}$ $s^{-1}$, an extensional strain of ~2 across the PRMB, as suggested by Ru & Pigott (1986), would require ~70 Ma, and strain 0.8 (Su *et al.* 1989) would require ~25 Ma. A lower extensional strain across the PRMB could in principle mean either a shorter duration or (more likely, given the constraints on timing) a lower strain rate.

### *Sediment supply*

Most PRMB sediment has been transported from the Chinese landmass by rivers, the most important being the Pearl (Zhu in Chinese) (Fig. 1). According to Milliman & Meade (1983), the Pearl drains 440,000 $km^2$ of area, which is mostly well below 1000 m elevation, and

Fig. 3. Cartoons summarizing relationships between the tectonic evolution of the Pearl River Mouth basin (PRMB) and its surroundings. Thick lines with paired arrows denote active left-lateral strike-slip faults, the Red River (RR) and Gulf of Thailand (GT) faults, which form transcurrent boundaries between the Eurasian plate (EU) and the Indochina and Malaya blocks (IC) and (MA). SI denotes the Spratley Islands plateau, a submarine plateau situated at present near the southeast coast of the South China Sea offshore of Borneo. Its shallow bathymetry indicates that it has experienced relatively little extension compared with its surroundings. Large dots denote the main localities that are actively extending at the time considered. Fine dots denote oceanic lithosphere in the central part of the South China Sea, with thick lines indicating active spreading centres. Short arrows facing away from each other indicate where extensional relative motion of EU, IC and MA was localized at the times considered. Fine dashed line indicates the extent of material that was at the earth's surface but is now removed, either by subduction beneath the Philippines or Borneo, or through some other process. (a) is at ~50 Ma, shortly after the Red River fault became active and active extension of the PRMB and its surroundings began. (b) is at 30 Ma, shortly after PRMB extension ceased, and relative motion between EU and IC became concentrated farther south near the oceanic spreading centre that was developing. (c) is at 20 Ma, by which time all extensional relative motion of EU and IC was apparently accommodated by oceanic spreading. Active spreading and left-lateral strike-slip ceased shortly afterwards. Information from Taylor & Hayes (1982) and Tapponnier *et al.* (1990).

Table 1. Simplified stratigraphy of the Pearl River Mouth Basin

| Formation | (1) Age (Ma) | (2) Age (Ma) | Environment |
|---|---|---|---|
| | 2–0 (Quaternary) | 2–0 (Quaternary) | Shallow marine |
| Wanshan | 5–2 (Pliocene) | 5–2 (Pliocene) | Shallow marine |
| Yehai | 11–5 (Late Miocene) | 11–5 (Late Miocene) | Shallow marine |
| Hanjiang | 14–11 (Middle Miocene) | 18–11 (Middle Miocene) | Deltaic |
| Zhujiang | 23–14 (Early Miocene) | 26–18 (Late Oligocene–Early Miocene) | Deltaic |
| Zhuhai | 35–23 (Oligocene) | 30–26 (Early–Late Oligocene) | Lagoonal |
| Enping | 43–35 (Late Eocene–Oligocene) | 36–30 (Early Oligocene) | Lacustrine |
| Wenchang | 55–43 (Eocene) | 40–36 (Late Eocene) | Lacustrine |
| Shenhu | 65–55 (Paleocene) | 50–40 (Early–Late Eocene) | Fluvial |

Ages in column (1) are from Chen & Li (1987), as used by Su *et al.* (1989). Ages in column (2) are based on revised sequence stratigraphic analysis by Edwards (1992). Note that the age interpretations diverge during Paleogene time, when absolute control from the global nannofossil time-scale is lacking.

Table 2. Normal faulting in the Pearl River Mouth Basin

| Fault | Dip polarity | $\delta$ (°) | $T$ (km) | $H$ (km) | $\theta$ (°) | $\delta_{o,1}$ (°) | $\delta_{o,2}$ (°) |
|---|---|---|---|---|---|---|---|
| 1 | SSE | 30 | 1.0 | 1.8 | 0 (H) | 30 | 30 |
| 2 | NNW | 23 | 1.0 | 2.4 | 7 (H) | 29 | 30 |
| 3 | SSE | 32 | 5.0 | 7.9 | 0 (H) | 32 | 32 |
| 4 | NNW | 27 | 3.0 | 5.8 | 8 (F) | 33 | 35 |
| 5 | NNW | 23 | 4.2 | 10.0 | 8 (H) | 29 | 31 |
| 6 | NNW | 20 | 3.2 | 8.8 | 18 (H) | 35 | 38 |
| 7 | SSE | 30 | 1.2 | 2.1 | 0 (H) | 30 | 30 |
| 8 | NNW | 30 | 6.0 | 10.4 | 0 (H) | 30 | 30 |
| Total | | | | 49.2 | | | |

$T$ and $\delta$ are present-day throw (vertical slip) and dip of normal faults, measured from the cross-section in Fig. 2. $H$ is heave (horizontal slip parallel to this cross-section), estimated as $T\cot(\delta)$. $\theta$ is tilt of top basement adjacent to each fault, measured from Fig. 2, towards the fault if in its hanging wall (H), or away from it if in its footwall (F). Su *et al.* (1989) used tilt values 12°, 15° and 30° for the blocks between faults 4–5, 5–6 and 6–7. $\delta_o$ is estimated initial dip of fault. Assuming rigid-body rotation, $\delta_o = \delta + \theta$. Assuming vertical shear, $\delta_o$ is given instead by $\tan(\delta_o) = \tan(\delta) + \tan(\theta)$ (Westaway & Kusznir 1993). Initial fault dip estimate $\delta_{o,1}$ is for vertical shear; $\delta_{o,2}$ is for rigid-body rotation.

carries $69 \times 10^9$ kg year$^{-1}$ of sediment to the sea. Taking the density of sediment particles as 2700 kg m$^{-3}$, this means a sediment volume of $\sim 30 \times 10^6$ m$^3$ year$^{-1}$, indicating spatial average net erosion rate over this drainage basin of $\sim$0.06 mm year$^{-1}$. If sustained over 60 Ma, the sediment flux in the Pearl river would require almost 4 km of erosion. If compensated isostatically, this requires $\sim$4 km of uplift. Given the $\sim 300 \times 800$ km dimensions of the PRMB, its 0.11 mm year$^{-1}$ sedimentation rate indicates sediment flux $\sim 26 \times 10^6$ m$^3$ year$^{-1}$, roughly 85% of the flux in the Pearl river.

The Red river (Hungho in Chinese, Songkoi in Vietnamese), which flows into the Gulf of Tongking farther west, drains 120,000 km$^2$ of area, mostly in elevated regions that have been uplifted by the collision of India and Eurasia that formed the Tibetan plateau. It carries $130 \times 10^9$ kg year$^{-1}$ (Milliman & Meade 1983) or $\sim 50 \times 10^6$ m$^3$ year$^{-1}$ of sediment, indicating typical net erosion rate over its drainage basin of $\sim$0.4 mm year$^{-1}$. This sediment presumably accumulates in the extensional basins in the western South China Sea. Similar dramatic erosion also occurs in much of southeast Asia (Milliman & Meade 1983).

These high erosion rates are caused by the climate. Coastal parts of China have typical rainfall $\sim$2000 mm year$^{-1}$, with amounts five times larger in more elevated regions inland. Most rainfall occurs in the summer monsoon, which carries moist air northward onto these landmasses. Numerical simulations indicate that the proximity of the Tibetan plateau to warm oceans has caused this unusual climate (e.g. Raymo & Ruddiman 1992). Similar climate and erosion may well have thus persisted since Eocene when this plateau began to form. This deduction is supported by the uniformity of PRMB sedimentation rates during Oligocene and younger time, which requires a uniform inward sediment flux.

### *Past estimates of extension*

Su *et al.* (1989) estimated the extension across the profile in Fig. 2 three ways. First, they used the rigid domino model (e.g. Jackson & McKenzie 1983) to estimate the extension taken up by normal faults in the brittle upper crust, giving an estimate $\beta_f$ for $\beta$ (Table 2). Second, assuming local conservation of crustal volume, they used the observed thinning of crustal basement to obtain an alternative estimate for $\beta$, $\beta_c$. Third, they obtained an estimate $\beta_s$ from subsidence within the basin. They used theory from McKenzie (1978), modified for a finite duration of extension, which assumes that isostatic compensation of extension, sedimentation, and thermal contraction of the lithosphere is by vertical displacement only. These three estimates all support $\beta \sim 1.8$ (Table 3).

This consistency of these $\beta$ estimates seems impressive. However, the analysis of faulting by Su *et al.* (1989) assumes that blocks within the brittle layer are infinitely rigid, and accommodate extension by rotating as rigid 'dominoes'. Their analysis of subsidence assumes instead that the brittle layer has no strength, such that isostatic compensation occurs in a pointwise (i.e. Airy) manner. Many recent studies have suggested that the brittle layer is neither infinitely rigid nor infinitely weak (e.g. King *et al.* 1988, Kusznir *et al.* 1991): it retains finite strength on geological time scales. Westaway (1992a) has developed a straightforward method for estimating long-term elastic moduli of the surroundings to normal faults that cut the brittle layer and take up substantial

Table 3. Analyses of extension across the Pearl River Mouth Basin

| Locality | A | B | C |
|---|---|---|---|
| *Observations* | | | |
| Present-day block width $W$ (km) | 45.5 | 68.2 | 83.3 |
| Present-day fault dip $\delta$ (°) | 23 ± 5 | 18 ± 5 | 27 ± 5 |
| Block tilt $\theta$ (°) | 12 ± 3 | 15 ± 3 | 30 ± 3 |
| Crustal basement thickness $T_b$ (km) | 19 ± 3 | 20 ± 3 | 14 ± 3 |
| Depth of base sediment $T_s$ (km) | 6 | 5 | 8 |
| Thickness of post-rift sediment (km) | 4 | 4 | 6 |
| *Derived parameters from Su* et al. (1989) | | | |
| $\beta_f$ | 1.5 ± 0.2 | 1.8 ± 0.3 | 1.8 ± 0.2 |
| $\beta_{s1}$ (extension only during 60–35 Ma) | 1.8 ± 0.2 | 1.7 ± 0.2 | 1.6 ± 0.3 |
| $\beta_{s2}$ (extension also during 25–11 Ma) | 1.9 ± 0.1 | 1.8 ± 0.1 | 2.0 ± 0.2 |
| $\beta_c$ | 1.6 ± 0.3 | 1.5 ± 0.3 | 2.2 ± 0.5 |
| Fault-derived extension $X_f$ (km) | 15.2 ± 4.0 | 30.3 ± 6.3 | 37.0 ± 5.1 |
| Subsidence-derived extension $X_{s1}$ (km) | 20.2 ± 2.8 | 28.1 ± 4.7 | 31.2 ± 9.8 |
| Subsidence-derived extension $X_{s2}$ (km) | 21.6 ± 1.3 | 30.3 ± 2.1 | 41.7 ± 4.2 |
| Thinning-derived extension $X_c$ (km) | 17.1 ± 5.3 | 22.7 ± 9.1 | 45.4 ± 8.6 |
| *Derived parameters from this study* | | | |
| Extension $H$ (km) (neglecting erosion) | 10.0 | 8.8 | 13.5 |
| Original crustal thickness $T_c$ (km) | 31 | 30 | 30 |
| Local fault-derived extension $\beta_{f1}$ | 1.28 | 1.15 | 1.19 |
| Local fault-derived extension $\beta_{f2}$ | 1.36 | 1.19 | 1.27 |
| Subsidence-derived extension $\beta_s$ | 1.31 | 1.25 | 1.46 |
| Weight-loss-derived extension $\beta_w$ | 1.26 | 1.25 | 1.47 |
| Loss of material by channel flow, $E_1$ (km) | 4 | 5 | 10 |
| Loss of material by channel flow, $E_2$ (km) | 4 | 4 | 6 |

From Su *et al.* (1989), $W$ is measured between footwall cutoffs for faults bounding each block, as specified by Jackson & McKenzie (1983) (faults 4 and 5 for block A; 5 and 6 for block B; and 6 and 8 for block C). $\beta_f$ is calculated as $\sin(\delta+\theta/\sin(\delta)$ (see e.g. Jackson & McKenzie 1983). $\beta_{s1}$ and $\beta_{s2}$ are estimated from subsidence analysis by Su *et al.* (1989), by matching estimated amounts of water-loaded subsidence to predictions assuming each extension history. $\beta_c$ is calculated at $T_c/T_b$, where $T_c$ is their assumed initial crustal thickness of 30 km. $X_f$ is calculated as $W - W/\beta_f$. $X_{s1}$ and $X_{s2}$ are derived as $W - W/\beta_{s1}$ and $W - W/\beta_{s2}$. $X_c$ is derived as $W - W/\beta_c$.

In this study, extension $H$ is the total observed heave of all the normal faults (from Table 2) exposed between footwall cutoffs within each block (i.e. fault 5 for block A, fault 6 for block B, faults 7 and 8 for block C). $T_c$ is estimated from $T_s$ and $T_b$ using (A1.19). $\beta_{f1}$ in each locality is estimated as $h/(W-H)$ and is thus not corrected for erosion. $\beta_{f2}$ in each locality is estimated as $W/[W - (H + \delta H)]$, which assumes heave $\delta H$ (2 km for blocks A and B; 4 km for C) has been lost by erosion of each footwall crest. $\beta_s$ and $\beta_w$ are estimated using (A1.17) and (A1.20) with $\rho_i = 0.8\rho_c$. $E_1$ is calculated using $\beta_{f2}$; $E_2$ is calculated using $\beta_w$.

extension. This typically leads to Young's modulus values of ~1 GPa, roughly 1% of typical short-term values for infinitesimal strain but still substantial.

A second problem concerns the assumption of rigid-body rotation of fault-bounded blocks. Block rotation is the traditional explanation of the saw-tooth topography that can develop between closely-spaced planar normal faults. However, the recent investigations already cited indicate that blocks between normal faults deform instead by vertical shear: saw-tooth topography can result from uniform vertical shear strain; lateral variations in tilting, between more widely-spaced normal faults, can result from laterally varying vertical shear strain (Westaway & Kusznir 1993). Tilting in the surroundings to any normal fault typically dies out no more than ~20 km away (e.g. Westaway 1992a). Normal-fault-bounded blocks in the PRMB have width up to ~80 km (Fig. 2), and are thus not expected to remain rigid even if narrower blocks do. Vertical shear in the surroundings to normal faults is supported by field investigations (e.g. Axen & Wernicke 1991, Westaway 1993), analysis of stress in the brittle layer (Westaway 1992a), and analysis of angular relations between fault and bed tilting in extensional basins (Westaway & Kusznir 1993).

### *Revised estimate of extension from heaves of normal faults*

Westaway & Kusznir (1993) showed that restoring saw-tooth topography assuming vertical shear can give different amounts of extension compared with predictions for rigid-body rotation of 'dominoes'. In their example, where 15° of bed tilting is restored on faults with 45° present-day dip, which were initially 10 km apart, vertical shear predicts ~20% more extension. As will become clear, for the PRMB (with typical fault dip now ~20–30°, bed tilt up to 18°, and fault spacing up to ~80 km) the extension predicted for vertical shear is instead less than half the alternative for rigid-body rotation.

Table 2 summarizes the extension across the eight normal faults in Fig. 2 with throw 0.5 km or greater, which can be assumed to cut the brittle layer. Their 49 km total observed heave is a lower bound for the

extension across this 260 km long profile. The resulting lower bound for extensional strain is thus 49/(260 − 49) or 0.23. Faults in Fig. 2 with throw less than 0.5 km contribute at most 1 km of extra heave, making a minimal difference to this estimate. Any contribution from other faults that are too small to cut the brittle upper crust is likely to be minimal, and is neglected (see e.g. Westaway 1992b).

In footwalls of some of these faults (most notably 4, 6 and 8) top basement appears truncated, presumably through local erosion. Simple geometry indicates that ~1 km thickness of basement has been lost in each case. Given the ~30° normal fault dips, the observed heave on each of faults 4, 6 and 8 is thus ~2 km less than the true heave. This increases the total heave across the profile to ~55 km, indicating extensional strain ~55/205 or ~0.27. Some erosion of footwalls of the other faults may also have occurred. Assuming 1 km of erosion in each case increases the estimated total extension to ~65 km, indicating extensional strain ~65/195 or −0.33. This is probably an overestimate, because some footwalls show no evidence for erosion. The estimated extensional strain across the eight faults in Fig. 2 is thus ~0.3, making $\beta_f$ ~1.3, with uncertainty conservatively assessed as ±0.05.

## INTERPRETATION OF SUBSIDENCE AND CRUSTAL THINNING

My above $\beta_f$ estimate for the PRMB is much less than the alternative of ~1.8 from the rigid-domino analysis by Su *et al.* (1989), and their $\beta_s$ and $\beta_c$ values from analysis of subsidence and thinning of crustal basement. Although Su *et al.* (1989) obtained consistent results of ~1.8 for $\beta$ using all three of their methods, the above analysis indicates that their estimate from faulting is much too high.

Vertical shear and rigid-body rotation cannot be distinguished using angular relations between fault and bed tilting in the PRMB, because the ~30–35° initial dips of faults (estimated from the ~0–18° tilts of their immediate surroundings) are very similar for both deformation styles (Table 2). However, several of its features, including the lateral variations of tilt between some major faults, the different amounts of uniform tilt between others, and the reversals of fault polarity, are not expected in a region containing rigid 'dominoes'. The resemblance of some blocks in Fig. 2 to dominoes would decrease if this cross-section were true to scale. The $\beta_f$ values from Su *et al.* (1989) used the ~12–30° tilts in Table 3, which (from Fig. 2) approach the maxima for each block. Smaller $\beta_f$ would result from using lower values in rigid domino analysis instead, matching the average tilt of each block.

These observations suggest, first, that the rigid domino method is unsuitable for the PRMB, and second, they indicate that if this method is used despite the objections to it, smaller tilt angles are appropriate, which reduce estimated $\beta_f$. Two reasons thus exist why $\beta_f$ values from Su *et al.* (1989) are too high. The consistency between their rigid domino $\beta_f$ estimate and their $\beta_c$ values from thinning and subsidence means that if their $\beta_f$ is too high then so are their $\beta_c$ and $\beta_s$. I will pursue the possibility that these other overestimates are caused by failure to account for outward lower-crustal flow.

Appendix 2 discusses the conditions for lower-crustal flow beneath extensional basins. Its sense depends on the lithostatic pressure anomaly $\delta P$ at the base of the brittle layer beneath a basin, compared with beneath its surroundings: positive $\delta P$ indicates outward; negative $\delta P$ indicates inward. In the absence of sedimentation or erosion, thinning of the brittle layer during extension will make $\delta P$ negative, causing inward flow. This will even out variations of crustal thickness, such that it is roughly uniform after extension. Gans (1987) indeed noted that crustal thickness after extension of the BRP is roughly uniform, even though some parts of it have extended much more than others, and Kruse *et al.* (1991) explained this in terms of inward lower-crustal flow. However, rapid influx of sediment into an extensional province and/or erosion of its surroundings will increase $\delta P$, making positive values—favouring outward flow—feasible instead.

Appendix 1 compares conventional theory for the isostatic response to extension with a revision incorporating outward lower-crustal flow. It shows that if all sediment in a basin isostatically compensates this flow, conventional analysis will underestimate the subsidence by a factor of $R_f$, which is ~1.7 for a young basin of several kilometres thickness. From equation (A1.21) with $R_f$ 1.7, $\beta$ estimated as 1.8 from subsidence without taking channel flow into account adjusts to ~1.35 in the limit with all sedimentation isostatically compensated by outward lower-crustal flow, similar to my estimate of 1.3 from faulting in the PRMB. The calculation of $R_f$ assumes that thermal subsidence is complete, which is not so for the PRMB. However, from fig. 6 of Su *et al.* (1989), for PRMB extension during 60–35 Ma, $\beta$ 1.8 would cause ~1.8 times as much subsidence to the present as $\beta$ 1.3, roughly matching $R_f$. The incomplete thermal subsidence of the PRMB thus appears to not significantly affect the expected adjustment to $\beta$ using equation (A1.21). These considerations indicate that the observed PRMB subsidence is consistent with $>\beta$ ~1.3 plus isostatic compensation of sedimentation by outward lower-crustal flow.

Following lower-crustal flow (whether inward or outward, or during or after extension) the crustal thinning factor $\beta_c$ (the ratio of initial to final thickness of crustal basement) gives no direct indication of the extension. The parameter $\beta_w$ (the ratio of initial to final weight of a crustal column, counting the basin fill as part of the final weight) can be defined instead (A1.20). If all sedimentation is isostatically compensated by outward lower-crustal flow, then $\beta_w$ gives a precise estimate of extension. An estimate for $\beta_s$, the extension factor from subsidence of a basin following outward lower-crustal flow, can also be derived, equation (A1.17). Subject to the approximations and assumptions in Appendix 1, this

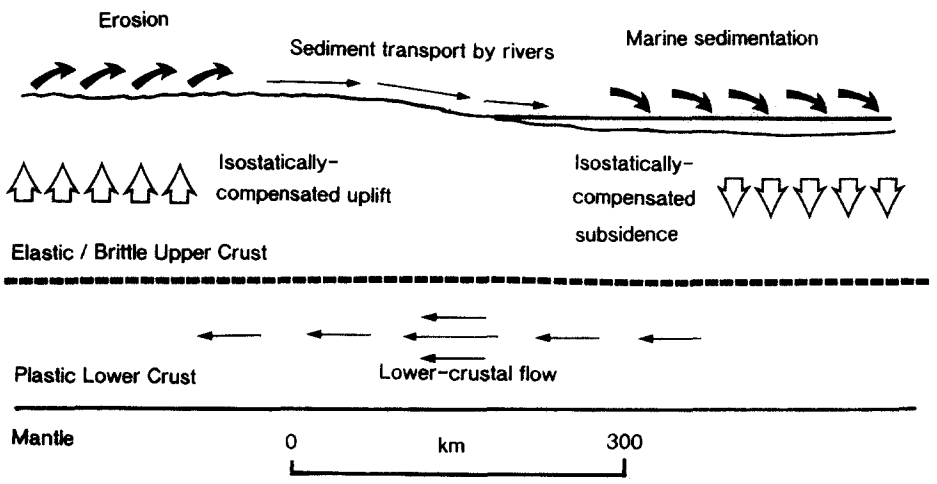


Fig. 4. Cartoon indicating schematically my suggested recycling of crustal material between the Chinese landmass and the Pearl River Mouth basin. The source of sediment is erosion from the Chinese landmass; its destination is the PRMB. The source of channel flow is beneath the PRMB; its destination or sink is beneath the Chinese landmass.

is also precise provided all sedimentation is isostatically compensated by this flow.

In Table 3, estimates of $\beta_s$ and $\beta_w$ for the PRMB are compared with my revised estimates of $\beta_f$, both local values and the value of 1.3 across the whole basin. When averaged across the profile in Fig. 2 both $\beta_c$ and $\beta_w$ are also ~1.3. The PRMB is thus indeed consistent with $\beta$ 1.3, with its weight of sediment balanced by at least 4 km loss of material from the lower crust.

*Destination of lower-crustal channel flow*

Previous calculations indicate that the volume fluxes of material eroded from the drainage basin of the Pearl river and deposited in the PRMB are roughly equal. This erosion and sedimentation have both occurred on a regional scale and will both be isostatically compensated. One may choose to believe that they are compensated independently, and their near equivalence is coincidental. Alternatively, this uplift and erosion may be isostatically compensated by lower-crustal material from beneath the PRMB.

This reasoning suggests that the cyclic process in Fig. 4 has occurred during PRMB sedimentation. As material erodes from the Chinese landmass and is transported seaward by rivers, this landmass uplifts isostatically. The eroded material is deposited in the PRMB, whose isostatic response requires loss of lower crustal material. This material flows landward through the lower crust, enabling the isostatic uplift of the Chinese landmass to occur in response to its erosion. Using equation (A3.5), to accommodate 0.1 mm year$^{-1}$ of isostatically compensated sedimentation or erosion by flow in a ~10 km deep lower-crustal channel with length ~300 km (the width of the PRMB) requires maximum horizontal flow velocity ~4.5 mm year$^{-1}$.

*Conditions for outward channel flow*

To address the likely timing of outward lower-crustal flow beneath the PRMB, consideration of the condition for this flow, positive $\delta P$, is necessary (Appendix 2). The natural point in time at which to begin is when extension ended. Assuming instantaneous extension, equation (A2.2) gives the critical thickness of sediment required by then for $\delta P$ to be positive. For $\beta = 1.3$, with initial thickness of the brittle layer 10 km, densities of sediment and crustal basement of 2200 and 2700 kg m$^{-3}$, it is only ~1.2 km. With a finite duration of extension, thermal conduction into the sedimentary column will reduce the depth of the base of the brittle layer. Greater sediment thickness is thus required to drive outward flow. However, given the short duration of PRMB extension, the difference is unlikely to be large.

The ~1.5 km average syn-rift sediment thickness in the PRMB thus slightly exceeds the estimated threshold for outward flow. It is thus likely that some outward flow did occur during extension, and the conditions at the end of extension thus favoured its continuation. The subsequent sedimentation is indeed expected to have driven most of the outward lower-crustal channel flow from beneath this basin.

The geothermal gradient in the PRMB is up to ~40°C km$^{-1}$ (Su *et al.* 1989), indicating that the base of the brittle layer is at ~10 km depth. If no thermal conduction had occurred during or after extension, with initial brittle layer thickness 10 km, the base of the brittle layer would typically be at $10/\beta$ km, or ~8 km depth. With ~5 km typical sediment thickness in the PRMB at present, the lithostatic pressure at 10 km depth will be ~240 MPa, equivalent to ~9 km thickness of basement. Thermal conduction has thus heated basement such that 3 km thickness of it that was originally in the brittle layer is now in the plastic lower crust. Assuming 10 km initial brittle-layer thickness beneath China and ~4 km loss of material by erosion, lithostatic pressure at the base of the brittle layer is greater at present beneath the PRMB than beneath the Chinese landmass, provided cooling of the brittle layer beneath China has not lowered its base by more than 3 km. If this condition for positive $\delta P$ continues to be satisfied then outward flow from beneath this basin is expected to continue to the present day.

Applying equation (A3.11) to the PRMB, with sedimentation rate 0.1 mm year$^{-1}$ and channel viscosity $10^{19}$ Pa s, $\delta P$ (time-averaged over the duration of flow) is 36 MPa for channel width 10 km, roughly 10% of the estimated lithostatic pressure at the base of the brittle layer. The required loss of material thus needs only a small lithostatic pressure anomaly, which cannot be excluded.

*Summary of PRMB extension*

This analysis estimates the extensional strain across the PRMB as 0.3, indicating $\beta = 1.3$. If the bulk of its extension occurred during 60–35 Ma, as suggested by Su *et al.* (1989), its time-averaged strain rate would be ~0.4 $\times$ $10^{-15}$ s$^{-1}$, indicating extension rate ~4 mm year$^{-1}$ across its ~300 km width. This interpretation is consistent with the timing of slip on the Red River fault from Tapponnier *et al.* (1990) and of sea-floor spreading in the South China Sea from Taylor & Hayes (1982) (Fig. 3). The alternative ~45–30 Ma timing of extension, consistent with the Edwards (1992) time scale, would instead indicate strain rate ~0.7 $\times$ $10^{-15}$ s$^{-1}$ or extension rate ~6 mm year$^{-1}$.

On its own, extension with $\beta$ 1.3 would thin the crust from ~30 to ~23 km. Channel flow is estimated to have typically removed at least 4 km of additional thickness, leaving <~19 km, as is observed (Fig. 2 and Table 3). The crust removed is interpreted as having flowed to beneath the Chinese landmass, where it has isostatically compensated the material that uplifted and eroded to form the sediment in the PRMB.

As already noted, PRMB sedimentation during deposition of the middle Miocene Hanjiang formation was faster than at any other time. Given that sedimentation in this basin appears to be isostatically compensated by outward lower-crustal channel flow, variations in its rate may indicate variations in rate of this flow, which may relate to variations in erosion rates related to climate. If so, the outward volume flux from beneath the PRMB was greatest during middle Miocene time.

Figure 2 indicates ~3.5 km average thickness of post-rift sediment in the PRMB. For $\beta = 1.3$, fig. 6 of Su *et al.* (1989) predicts water-loaded subsidence ~1.1 km during extension over 60–35 Ma, followed by ~0.2 km water-loaded thermal subsidence since extension ceased at 35 Ma. Using equation (A1.6) with $\rho_i$, the density of basin fill, equal to $\rho_w$, the density of water (~1000 kg m$^{-3}$), total water-loaded subsidence ~1.6 km is expected for $\beta = 1.3$ when thermal subsidence is complete. Only ~40% (0.2 km/(~1.6 km − 1.1 km)) of the expected thermal subsidence has thus so far occurred. The ~0.2 km water-loaded thermal subsidence expected since ~35 Ma indicates ~0.5 km sediment-loaded subsidence [~0.2 km $\times$ $(\rho_m - \rho_w)/(\rho_m - \rho_i)$, with $\rho_i$ ~2200 kg m$^{-3}$]. Most (~3 km out of 3.5 km) of the post-rift sediment-loaded subsidence of the PRMB is thus evidently not thermal subsidence. As already discussed, it is presumably associated instead with the isostatic compensation of outward lower-crustal channel flow. It is thus now clear why equation (A1.17) successfully interrelates subsidence and extension for this basin, even though its derivation assumes thermal subsidence is complete. Thermal contraction of the lithosphere as its temperature gradient returns to equilibrium has such a small effect on elevation changes in this basin that it makes little difference however naïvely it is approximated.

## DISCUSSION

*Tests for lower-crustal channel flow*

The suggestion that outward lower-crustal channel flow can accompany or follow extension can be tested in several ways. The first test considers whether it is mechanically feasible. This means whether the viscosity of the lower crust is low enough to allow flow at the required rates and whether the surroundings to the flow can withstand the resulting viscous forces. Appendix 3 derives equations for use in this test.

PRMB sedimentation (~3.5 km since ~35 Ma) indicates time-averaged rate ~0.1 mm year$^{-1}$. For ~300 km basin width, and ~10 km thickness of the plastic lower crust beneath it, from equation (A3.5) the required maximum horizontal flow velocity is ~4.5 mm year$^{-1}$. The average horizontal flow velocity at the landward margin of the basin is two-thirds of this value or ~3 mm year$^{-1}$. From equation (A3.7) the horizontal viscous force $F_x$ acting on each boundary of the channel is ~$10^{11}$ N m$^{-1}$ for lower-crustal viscosity $\eta$ ~$10^{19}$ Pa s. These estimates of velocity and $F_x$ are also time-averages since 35 Ma. The required $F_x$ value is an order-of-magnitude less than the threshold of ~$10^{12}$ N m$^{-1}$ that can be withstood by the strong parts of the continental lithosphere (see Kusznir 1991, also Appendix 3). There is thus no objection on mechanical grounds to the horizontal velocities of outward channel flow from beneath the PRMB of several mm year$^{-1}$, which are required to isostatically compensate its sedimentation.

A second test involves examination of the relevant equations (such as equation A3.13) to see under what circumstances outward lower-crustal channel flow is expected to have greatest volume flux if $\delta P$ is large, channel thickness $W$ is large, channel viscosity is small, or channel length is small. $W$ is constrained above by the base of the brittle layer and below by the base of the crust, and will be largest if initial crustal thickness is large. If $\beta$ is large, $W$ will decrease during extension and will be small after extension, inhibiting flow. If extension is slow, conduction of heat into the sedimentary column will raise the base of the brittle layer. This will slightly increase $W$, but will also substantially decrease $\delta P$, such that overall outward flow is inhibited. As already noted, if erosion of a basin's surroundings is rapid, outward flow will be encouraged. From equation (A2.2) a given amount of sedimentation is expected to have greatest effect on channel flow if brittle layer thickness is initially low, which means high initial heat

flow. Overall, from these considerations the volume flux of outward channel flow following extension is expected to be greatest where extension has been rapid, sedimentation and/or erosion of a basin's surroundings are rapid, initial crustal thickness is large, initial brittle layer thickness is small, or the overall extensional strain is small.

A third test examines when outward channel flow has the greatest overall effect on the form of a basin. From equation (A1.16), a given amount of extension will cause greater subsidence by factor $R_f$ if sedimentation isostatically compensates outward channel flow compared with if it does not. $R_f$ depends on the average density of basin fill $\rho_i$, such that larger $\rho_i$ means larger $R_f$. The overall effect of outward flow is thus greatest on the form of basins with large $\rho_i$. Large $\rho_i$ occurs when basin sediment is well-lithified, whether through compaction (for thick basins) or other processes such as diagenesis (for ancient basins).

A final test considers when lower-crustal channel flow is most efficient. The cycle described in Fig. 4 can be regarded as a machine that extracts gravitational potential energy from sediment as it subsides in a basin, using it to do work uplifting the eroding surroundings to the basin. Some work is of course also done in plastically deforming the lower crust. The efficiency of this machine, like any other, can be regarded as the ratio of useful work output to energy input. Appendix 4 investigates flow efficiency. For parameters appropriate to the PRMB the work done plastically deforming the lower crust is <10% of that done uplifting this basin's surroundings. Inspection of (A4.10) indicates that efficiency of lower-crustal channel flow decreases as volume flux and viscosity increase. For a given volume flux and viscosity, efficiency is greatest when the dimensions of the sedimentary basin and its eroding surroundings are small, or when the brittle layer and/or lower-crustal channel are thick.

Although energy losses deforming the lower crust are small, flow from beneath the PRMB is by no means 100% efficient. Because the sediment flux deposited in the PRMB is only ~85% of that eroded from the drainage basin of the Pearl river, overall this process is only ~85% efficient. The missing sediment is presumably deposited elsewhere, for example on the oceanic lithosphere in the central South China Sea where loading will not drive lower-crustal flow. An additional requirement for high efficiency of outward flow from beneath a sedimentary basin is thus the existence of a closed system, with ideally all sediment eroded from the basin's surroundings being deposited in its interior.

Many effects of a given amount of extension accompanied by outward lower-crustal channel flow thus mimic effects of greater extension without this flow. For instance, outward flow will thin the lower crust beneath a basin, causing $\beta_c$ to exceed true $\beta$. Isostatic compensation of outward flow will involve subsidence and sedimentation that mimic effects of larger $\beta_s$ (A1.16). Subsidence and thinning, modelled conventionally, will thus overestimate extension compared with faulting for any basin from which outward flow has been significant. By thinning the lower crust, outward flow will also raise its geothermal gradient, increasing heat flow into the upper crust and mimicking the heat flow expected conventionally for larger $\beta$. This will raise the temperature at the base of the brittle layer, causing it to migrate upward. It thus provides a negative feedback mechanism that may regulate the volume flux of outward lower-crustal channel flow. This flow is most efficient when it is slow, with a low volume flux, when the necessary conditions are only marginally satisfied (see above). This negative feedback may thus maintain it in regimes where energy losses in deforming the lower crust are minimized.

### *Evidence for outward channel flow beneath other extensional basins*

Following the widespread acceptance of McKenzie's (1978) stretching model and its derivatives, it has become standard to regard sedimentation in extensional basins that post-dates their extension as the result of thermal subsidence. However, the above analysis indicates that only a small fraction of the post-rift sedimentation in the PRMB can be attributed to this cause. Pending a systematic survey of other basins to estimate effects of outward lower-crustal channel flow on sediment thickness, indiscriminate use of the term 'thermal subsidence sediment' in lieu of 'post-rift sediment' should be discouraged.

It is easy to identify effects attributable to outward lower-crustal channel flow beneath other extensional basins that are bounded by eroding landmasses. An example is the northern North Sea, where most extension occurred in Triassic to late Jurassic or early Cretaceous time (~210–140 Ma). Figure 1 of Westaway & Kusznir (1993) shows a typical cross-section through this ~300 × ~300 km extensional province. Observed heaves of major normal faults total ~60–80 km, indicating $\beta_f \cong 300/220$ or = 1.4 (e.g. Marsden *et al.* 1990, Marrett & Allmendinger 1992). Correction for footwall erosion, which may conceal ~20 km more heave, raises $\beta_f$ to ~1.5. In the ~70 km wide Viking graben, the central part of this extensional province, the base of the crust is typically ~12 km, of which ~6 km is post-rift; typical sediment thickness is ~10 km, with ~5 km post-dating the extension. Localities flanking the Viking graben typically have less sediment thickness. Using (A2.2) with $\beta = 1.5$, the critical syn-rift sediment thickness required for outward flow is 4 km, slightly less than the typical thickness in the Viking graben. It thus appears likely that outward flow did occur during (and after) its extension. Using (A1.19), initial crustal thickness is estimated as ~33 km.

Conventional analysis using (A1.6) with $\beta = 1.5$ predicts only ~5.5 km of sediment, less than the observed thickness which requires $\beta_s$ ~2.5. 'Extension discrepancies' like this, between values of $\beta_f$ and conventional estimates of $\beta_c$ or $\beta_s$, have previously been reported in the North Sea. For instance, Ziegler (1983) estimated that $\beta_f$ for the Central graben is no greater

Table 4. Importance of outward channel flow for different extensional provinces

| Province | $T_c$ (km) | $\beta$ | $t$ (Ma) | $J$ (km) | $L$ (km) | $c$ (mm/year$^{-1}$) | $E$ (km) | $L_e$ (km) | $u$ (mm/year$^{-1}$) | $U$ (km) | $V$ (mm/year$^{-1}$) | $Q$ (km$^3$/year$^{-1}$) | $E/(T_c-T_c/\beta)$ |
|---|---|---|---|---|---|---|---|---|---|---|---|---|---|
| Michigan (now) | 30 | 1.03 | 150 | 500 | 600 | 0.02 | 3 | | | | 1.8 | 0.006 | 2.6 |
| Michigan (400 Ma) | 30 | 1.03 | 50 | 500 | 600 | 0.03 | 1.5 | | | | 2.7 | 0.009 | 1.7 |
| PRMB | 30 | 1.3 | 35 | 800 | 300 | 0.10 | 4 | 300 | 0.08 | 4 | 4.5 | 0.024 | 0.6 |
| Viking graben | 33 | 1.5 | 140 | 300 | 70 | 0.06 | 9 | 500 | 0.01 | 1 | 0.6 | 0.001 | 0.8 |

$\beta$ and $t$ are the estimated extension factor and duration of channel flow; $T_c$ is the calculated (or assumed—see text) initial crustal thickness; $L$ and $L_e$ are the lengths of the lower-crustal channel beneath the source and sink of lower-crustal flow (the width of the extensional province and the eroding landmass from which its sediment is derived); $J$ is the along-strike length of the extensional province; $c$ and $E$ are the rate of loss and total loss of crustal basement by channel flow; $u$ and $U$ are the uplift rate and total uplift at this sink; $V$ is maximum channel flow velocity, from (A3.5), assuming 10 km thickness of the lower-crustal channel; $Q$ ($=c\,L\,J$) is the estimated volume flux of this flow; $T_c - T_c/\beta$ is the thickness of crustal basement lost by extension, so $E/(T_c - T_c/\beta)$ is the ratio of thickness of crustal basement lost by channel flow to that lost by extension. For the Viking graben, channel flow is assumed bidirectional; for the PRMB it is assumed unidirectional towards China. For both, the duration of the bulk of channel flow is taken as the time since extension ceased. Uplift of regions flanking the Michigan basin is not quantified, because the appropriate dimensions are unclear.

than 1.15, but $\beta_c$ and $\beta_s$ are no less than ~1.5. These discrepancies have been explained in various ways, including loss of lower-crustal material (Ziegler & Van Hoorn 1989). Marrett & Allmendinger (1992) instead regarded the cumulative effect of minor faults as the cause, while White (1990) claimed that there is no discrepancy given the uncertainties in individual estimates.

The surroundings to the North Sea now comprise the landmasses of Scotland and Norway, which uplifted above sea level during early Tertiary time. Erosion from Scotland has provided much of the Tertiary sediment in the western part of the North Sea (e.g. Glennie 1986, pp. 189–194). Average elevation is now ~500 m for ~200 km width of Scotland and ~1 km for ~300 km width of Norway. With present-day crustal basement thickness 13 km and $\beta = 1.5$, equation (A1.18) gives the typical thickness of material lost from beneath the Viking graben as ~9 km, sufficient to uplift Scotland and Norway on average by ~1 km. Outward lower-crustal channel flow can thus explain the present-day forms of the North Sea, Scotland, and Norway, following extension with $\beta$ ~1.5. Using equation (A1.17), sediment thickness 10 km gives $\beta_s$ ~1.6 for the Viking graben, virtually the same as $\beta_f$ across the northern North Sea as a whole. The much greater subsidence of the Viking graben compared with flanking regions may thus reflect loss of lower-crustal material, rather than indicating substantially greater local extension.

Other extension discrepancies are provided by the various Paleozoic basins within the North American landmass, such as Williston, Illinois, and Michigan, where despite substantial subsidence there is only minimal evidence of faulting. Various *ad hoc* explanations exist for this apparently anomalous form (see e.g. the review by Allen 1992). The ~500 km long and ~600 km wide Michigan basin has post-Precambrian sediment thickness up to ~4 km (e.g. Sleep & Sloss 1980), most of which accumulated during ~450–300 Ma. Using $\rho_i$ ~2600 kg m$^{-3}$, for ancient well-lithified sediment, conventional analysis using (A1.6) gives $\beta_s$ ~1.2, indicating ~100 km of extension. Using (A1.17) instead gives $\beta_s$ ~1.03, requiring only ~20 km of extension.

Table 4 summarizes channel-flow interpretations of the PRMB, the Viking graben, and the Michigan basin. The latter is interpreted both at present and at ~400 Ma, when ~1.5 km equivalent thickness of consolidated sediment already existed. In all cases the estimated crustal basement thinning caused by outward flow is substantial compared with that caused directly by extension: 4 km against 7 km for the PRMB; 9 km against 11 km for the Viking graben; and 3 km against 1 km for the Michigan basin. The analysis of the Michigan basin indicates that the outward volume flux was largest during the earliest stages of sedimentation, but significant time-averaged flux persisted for ~150 Ma. By analogy, outward flow may persist for many Ma from beneath the PRMB, causing additional crustal basement thinning in the future. Comparison of the Michigan basin and the Viking graben supports the deduction from inspection of equations that outward flow has greatest effect on the overall form of a basin where extensional strain is small. Despite its large outward volume flux and lower $\beta$ value, outward flow appears to have had less effect on the form of the PRMB than on the Viking graben. This is presumably because of the reduction in efficiency caused by loss of some of the sediment eroded from the surroundings of the PRMB.

### *Comparison with inward channel flow in the Basin and Range province*

The most detailed previous investigation of lower-crustal channel flow is probably by Kruse *et al.* (1991). Following a suggestion by Wernicke (1990), they investigated whether inward flow beneath the BRP may cause uniform crustal thickness despite strong lateral variations in extension. They determined the duration $\delta t$ of the flow required to eliminate an initial negative lithostatic pressure anomaly $\delta P$. Using my notation (noting that their length parameter $L$ covers the length of the source and sink of channel flow, and thus equals $L + L_e$ in my notation; for symmetrical flow with $L = L_e$, their parameter is thus double my $L$), their equation (5) can be written as

$$\delta_t = \frac{12L^2\eta}{W^3\rho_c g} \quad (1)$$

which is similar to (A3.11). Comparison indicates that $\delta t = c\ (\delta P/\rho_c\ \mathbf{g})$. $\delta t$ thus validly estimates the time needed to eliminate, by channel flow with $c$ uniform over time, the thickness of crust $\delta p/\rho_c g$ that supports the initial lithostatic pressure anomaly. Both sets of equations are thus consistent, but mine are in a form better suited to describing flow maintained by sedimentation and erosion, rather than flow driven by initial conditions.

The BRP has overall $\beta$ of at least 2 (e.g. Gans 1987, Wernicke *et al.* 1988), and has not experienced much influx of sediment from erosion of its surroundings. Given earlier discussion, it is reasonable for its channel flow to be inward. There is thus no conflict between my results and those of Kruse *et al.* (1991): the sense of lower-crustal channel flow beneath any extensional province depends on its conditions. The different senses of this flow may indeed be the main cause of the dramatically different present-day forms of the BRP and PRMB, which both experienced early Tertiary extension.

Inward flow has the opposite implications for systematic errors in extension from subsidence and crustal thinning compared with outward flow: conventional analyses will underestimate extension. The typical ~30 km present-day crustal thickness within the BRP (e.g. Allmendinger *et al.* 1987) and the $\beta$ value of no less than 2 do not mean initial crustal thickness at least 60 km. The popular view that BRP extension has been caused by collapse of overthickened continental crust thus may well not be correct.

### *Implications for other localities*

The analyses in Appendices 3 and 4 are not restricted to lower-crustal channel flow during or after extension. In stable regions, any locality receiving sediment can in principle be a source of such flow; any locality that is eroding can in principle be a sink. This flow will in general act to even out irregularities in crustal thickness, and may well be the general process that maintains the continental crust at its uniform ~30 km thickness. Many other structural settings may indeed exist where failure in the past to address this flow may have caused systematic errors in interpretation. For instance, localities undergoing crustal shortening and thickening can be expected to experience outward flow in the lower crust. In localities where thinning of the continental crust reduces its thickness below the typical brittle-layer thickness of ~10–20 km, the entire crust may be within the brittle regime, with no lower-crustal channel. Channel flow thus cannot occur beneath passive margins that have undergone extreme extension, and thus cannot enable these localities to recover their original crustal thickness.

## CONCLUSIONS

The extension factor across the Pearl River Mouth Basin has been reinterpreted as 1.3 ±0.05 using normal fault heaves. This is thus much less than previous estimates of ~1.8 for this basin, from conventional analysis of subsidence and crustal thinning by Su *et al.* (1989). Its observed subsidence and crustal basement thinning are consistent with my revised extension factor, plus outward lower-crustal channel flow that has removed at least 4 km of crustal thickness. It is suggested that this material flows beneath the adjacent Chinese landmass to maintain isostatic equilibrium during the erosion that supplies sediment to the PRMB. Most flow is estimated to have occurred after extension ceased around 35 Ma.

The possibility of lower-crustal channel flow means that the interpretation of subsidence in extensional basins is much more difficult than was previously thought. Such flow may occur during or after extension, and may be either inward or outward. Outward flow is likely to be most important for rapid extension, sedimentation, or erosion of a basin's surroundings. It may provide the key to understanding discrepancies in extension when subsidence is compared with faulting for other basins also. In localities where outward flow is significant, conventional subsidence analysis systematically overestimates extension.

*Acknowledgements*—This work was supported by private funds. I thank Joel Watkins and Sue Treagus for constructive reviews.

## REFERENCES

Allen, C. R., Gillespie, A. R., Han, Y., Sieh, K. E., Zhang, B. and Zhu, C. 1984. Red River and associated faults, Yunnan Province, China: Quaternary Geology, slip rates, and seismic hazard. *Bull. geol. Soc. Am.* **95**, 686–700.

Allen, P. 1992. Review of "Interior Cratonic basins, AAPG memoir 51, 819 pp." *Basin Res.* **3**, 245–247.

Allmendinger, R. W., Hauge, T. A., Hauser, E. C., Potter, C. J., Klemperer, S. L., Nelson, K. D., Knuepfer, P. & Oliver, J. 1987. Overview of the COCORP 40°N transect, western United States: the fabric of an orogenic belt. *Bull. geol. Soc. Am.* **98**, 308–319, 1987.

Axen, G. J. & Wernicke, B. P. 1991. Comment on "Tertiary extension and contraction of lower-plate rocks in the central Mojave metamorphic core complex, southern California" by Bartley, J. M., Fletcher, J. M. & Glazner, A. F. *Tectonics* **10**, 1084–1086.

Chen, S. & Li, Z. 1987. Major oil accumulation characteristics and exploration direction in the Pearl River Mouth basin. In: *Proceedings of the International Symposium on Petroleum Geology of the Northern Continental Shelf of the South China Sea.* Guangdong Petroleum Society and China Oil, Guangzhou, 12–23.

Edwards, P. B. 1992. Structural evolution of the western Pearl River Mouth basin. In: *Geology and Geophysics of Continental Margins* (edited by Watkins, J. S., Feng, Z. & McMillen, K. J.). *Mem. Am. Ass. Petrol. Geol.* **53**, 43–52.

Feng, Z., Miao, W., Zheng, W. & Chen, S. 1992. Structure and hydrocarbon potential of the para-passive Continental margin of the northern South China Sea. In: *Geology and Geophysics of Continental Margins* (edited by Watkins, J. S., Feng, Z. & McMillen, K. J.). *Mem. Am. Ass. Petrol. Geol.* **53**, 27–41.

Funahara, S., Nishiwaki, N., Murata, F., Otofuji, Y. & Wang, Y. 1993. Clockwise rotation of the Red River fault inferred from paleomagnetic study of Cretaceous rocks in the Shan-Thai-Malay block of western Yunnan, China. *Earth Planet. Sci. Lett.* **117**, 29–42.

Gans, P. B. 1987. An open-system, two-layer crustal stretching model for the eastern Great Basin. *Tectonics* **6**, 1–12.

Glennie, K. W. 1986. *Introduction to the Petroleum Geology of the North Sea* (2nd edn). Blackwell Scientific, Oxford.

Jackson, J. A. & McKenzie, D. P. 1983. The geometrical evolution of normal fault systems. *J. Struct. Geol.* **5**, 471–482.

Jackson, J. A. & McKenzie, D. P. 1988. The relationship between plate motions and seismic moment tensors, and the rates of active deformation in the Mediterranean and Middle East. *Geophys. J.* **93**, 45–73.

King, G. C. P., Stein, R. S. & Rundle, J. B. 1988. The growth of geological structures by repeated earthquakes: 1. Conceptual framework. *J. geophys. Res.* **93**, 13,307–13,318.

Kruse, S., McNutt, M., Phipps-Morgan, J., Royden, L. & Wernicke, B. 1991. Lithospheric extension near Lake Mead, Nevada: a model for ductile flow in the lower crust. *J. geophys. Res.* **96**, 4435–4456.

Kusznir, N. J. 1991. The distribution of stress with depth in the lithosphere: thermo-rheological and geodynamic constraints. *Phil. Trans. R. Soc. Lond.* **A337**, 95–110.

Kusznir, N. J., Marsden, G. & Egan, S. S. 1991. A flexural cantilever simple shear/pure shear model of continental lithosphere extension: applications to the Jeanne d'Arc basin, Grand Banks, and Viking graben, North Sea. In: *The Geometry of Normal Faults* (edited by Roberts, A. M., Yielding, G. & Freeman, B.). *Spec. Publs geol. Soc. Lond.* **56**, 41–60.

Kusznir, N. J. & Park, R. G. 1987. The extensional strength of the continental lithosphere: its dependence on geothermal gradient, and crustal composition and thickness. In: *Continental Extensional Tectonics* (edited by Coward, M. P., Dewey, J. F. & Hancock, P. L.). *Spec. Publs geol. Soc. Lond.* **28**, 35–52.

Marrett, R. & Allmendinger, R. W. 1992. Amount of extension on "small" faults: an example from the Viking graben. *Geology* **20**, 47–50.

Marsden, G., Yielding, G., Roberts, A. M. & Kusznir, N. J. 1990. Application of a flexural cantilever simple shear/pure shear model of continental lithosphere extension to the formation of the northern North Sea basin. In: *Tectonic Evolution of the North Sea Rifts* (edited by Blundell, D. J. & Gibbs, A. D.). Oxford University Press, Oxford, 236–257.

McKenzie, D. P. 1978. Some remarks on the development of sedimentary basins. *Earth Planet. Sci. Lett.* **40**, 25–32.

Milliman, J. D. & Meade, R. H. 1983. Worldwide delivery of river sediment to the oceans. *J. Geol.* **91**, 1–21.

Peltier, R. 1982. Dynamics of the ice-age earth. *Adv. Geophys.* **24**, 1–146.

Raymo, M. E. & Ruddiman, W. F. 1992. Tectonic forcing of late Cenozoic climate. *Nature* **359**, 117–122.

Reilinger, R. 1986. Evidence for postseismic viscoelastic relaxation following the 1959 M = 7.5 Hebgen Lake, Montana, earthquake. *J. geophys. Res.* **91**, 9488–9494.

Ru Ke, & Pigott, J. D. 1986. Episodic rifting and subsidence in the South China Sea. *Bull. Am. Ass. Petrol. Geol.* **70**, 1136–1155.

Sleep, N. H. & Sloss, L. L. 1980. The Michigan basin. In: *Dynamics of Plate Interiors* (edited by Bally, A. W., Bender, P. L., McGetchin, T. R. & Walcott, R. I.). *Am. Geophys. Un. Geodyn. Ser.* **1**, 93–98.

Su, D., White, N. J. & McKenzie, D. P. 1989. Extension and subsidence of the Pearl River Mouth basin, northern South China Sea. *Basin Res.* **2**, 205–222.

Tapponnier, P., Lacassin, R., Leloup, P. H., Schärer, U., Zhong, D., Wu, H., Liu, X., Ji, S., Zhang, L. & Zhong, J. 1990. The Ailao Shan/Red River metamorphic belt: Tertiary left-lateral shear between Indochina and south China. *Nature* **343**, 431–437.

Taylor, B. & Hayes, D. E. 1982. Origin and history of the South China Sea basin. In: *The Tectonic and Geologic Evolution of Southeast Asian Seas and Islands. Am. Geophys. Un. Geophys. Monogr.* **27**, part 2, 23–56.

Turcotte, D. L. & Schubert, G. 1982. *Geodynamics: Applications of Continuum Physics to Geological Problems*. Wiley, New York.

Wang, S., Xie, T., Wang, S. & Liu, L. 1992. Geological characteristics and petroleum potential of sedimentary basins of the China continental shelf. In: *Geology and Geophysics of Continental Margins* (edited by Watkins, J. S., Feng, Z. & McMillen, K. J.). *Mem. Am. Ass. Petrol. Geol.* **53**, 3–16.

Wernicke, B. 1990. The fluid crustal layer and its implications for continental dynamics. In: *Exposed Cross-sections of the Continental Crust* (edited by Salisbury, M. H. & Fountain, D. M.). Kluwer, The Netherlands, 509–544.

Wernicke, B., Axen, G. J. & Snow, J. K. 1988. Basin and range extensional tectonics at the latitude of Las Vegas, Nevada. *Bull geol. Soc. Am.* **100**, 1738–1757.

Westaway, R. 1992a. Analysis of tilting near normal faults using calculus of variations: implications for upper crustal stress and rheology. *J. Struct. Geol.* **14**, 857–871.

Westaway, R. 1992b. Evidence for anomalous earthquake size distributions in regions of minimal strain. *Geophys. Res. Lett.* **19**, 1499–1502.

Westaway, R. 1993. Neogene evolution of the Denizli region of western Turkey. *J. Struct. Geol.* **15**, 37–53.

Westaway, R. & Kusznir, N. J. 1993. Fault and bed 'rotation' during continental extension: block rotation or vertical shear? *J. Struct. Geol.* **15**, 753–790 (with 1993 correction: *J. Struct. Geol.* **15**, 1391).

White, N. J. 1990. Does the uniform stretching model work in the North Sea? In: *Tectonic Evolution of the North Sea Rifts* (edited by Blundell, D. J. & Gibbs, A. D.). Oxford University Press, Oxford, 217–239.

Ziegler, P. A. 1983. Crustal thinning and subsidence in the North Sea. *Nature* **304**, 561.

Ziegler, P. A. & Van Hoorn, B. 1989. Evolution of the North Sea rift. In: *Extensional Tectonics and Stratigraphy of the North Atlantic Margin* (edited by Tankard, A. J. & Balkwill, H. R.). *Mem. Am. Ass. Petrol. Geol.* **46**, 471–500.

## APPENDIX 1
## LITHOSPHERE DEFORMATION DURING EXTENSION

This Appendix summarizes conventional theory for the isostatic response to lithosphere extension, presents new theory incorporating isostatic compensation by outward channel flow, and compares the predictions of both forms of theory.

### *Conventional theory for isostatic response during lithosphere extension*

The conventional theory for the isostatic response of the lithosphere to extension was developed by McKenzie (1978). He analyzed instantaneous extension throughout the lithosphere by factor $\beta$ with volume balanced by upwelling of the asthenosphere, followed by cooling as the lithosphere returns to thermal equilibrium. Isostatic compensation of crustal–basement subsidence and sedimentation is assumed to be by vertical deflection of the Moho. This theory was developed before the importance of depth-dependent variations in lithosphere rheology were recognized: the upper crust is brittle and deforms by faulting; the lower crust and mantle lithosphere are plastic; the lower crust is much weaker than the mantle lithosphere due to its different composition (e.g. Kusznir & Park 1987, Wernicke 1990).

Let $\rho_c$ and $\rho_m$ denote the average densities of crust and mantle lithosphere, $\rho_a$ and $\rho_i$ denote the density of asthenosphere and average density of fill of an extensional basin (water or sediment), and $T_c$ and $T$ denote the initial thickness of the crust and lithosphere. The initial weight of a column of lithosphere is proportional to $[T_c \rho_c + (T - T_c) \rho_m]$. Suppose that as the lithosphere extends instantaneously by factor $\beta$, the asthenosphere upwells by distance $T_a$ and the Earth's surface subsides by distance $S_s$. The thickness of the column of extended lithosphere and upwelled asthenosphere is $(S_s + T/\beta + T_a)$; its weight is proportional to $[S_s \rho_i + T_c \rho_c/\beta + (T - T_c) \rho_m/\beta + T_a \rho_a]$. McKenzie (1978) deduced $S_s$ by solving simultaneously the equations for lithosphere thickness and isostatic equilibrium before and after extension,

$$T = S_s + T/\beta + T_a \tag{A1.1}$$

and

$$T_c\rho_c + (T - T_c)\,\rho_m = S_s\rho_i + T_c\rho_c/\beta + (T - T_c)\rho_m/\beta + T_a\rho_a \tag{A1.2}$$

to give:

$$S_s = (1 - 1/\beta)\,\frac{T_c(\rho_m - \rho_c) - T\,(\rho_m - \rho_a)}{\rho_a - \rho_i}. \tag{A1.3}$$

After extension, the asthenospheric material that has upwelled will cool and become incorporated into the lithosphere. Long afterward, the lithosphere will return to thermal equilibrium. An approximate solution for the total subsidence $S_f$ when this equilibrium is achieved can be obtained by assuming that the average density of the crust and mantle lithosphere are the same as before extension began. Let the final thickness of mantle lithosphere be $T_m$. The thickness of the column of extended lithosphere is thus $(S_f + T_c/\beta + T_m)$, and its weight is proportional to $(S_f \rho_i + T_c \rho_c/\beta + T_m \rho_m)$, so

$$T = S_f + T_c/\beta + T_m \tag{A1.4}$$

and

$$T_c\rho_c + (T - T_c)\rho_m = S_f\rho_i + T_c\rho_c/\beta + T_m\rho_m \quad \text{(A1.5)}$$

or

$$S_f = (1 - 1/\beta)\frac{T_c(\rho_m - \rho_c)}{\rho_m - \rho_i}. \quad \text{(A1.6)}$$

These equations, derived from this approximate treatment of McKenzie's (1978) model, can be compared with more precise versions. For example, a more accurate expression for $S_f$ is (in my notation)

$$S_f = (1 - 1/\beta)\frac{T_c(\rho'_m - \rho'_c)}{\rho_a - \rho_i} \quad \text{(A1.7)}$$

(see e.g. Su *et al.* 1989) where $\rho'_m$ and $\rho'_c$ are the density of crust and mantle lithosphere at 0°C. These exceed the average densities $\rho_m$ and $\rho_c$ in (A1.6) by a few percent, but these differences largely cancel after subtraction. $\rho_a$ in (A1.7) is also a few percent less than $\rho_m$ in (A1.6). Equation (A1.6) is thus a good approximation to (A1.7).

*Modification to incorporate lower-crustal flow*

McKenzie's (1978) theory and its derivatives assume that loading of the crust is accommodated by downward deflection of the Moho to maintain isostatic equilibrium, and volume of crustal basement is locally conserved in each part of an extensional province. As discussed in the main text, some of the lower crust may flow horizontally out of an extensional province, causing a loss of volume that affects overall isostatic equilibrium. Full treatment of this equilibrium during and after extension when part of the lower crust is lost is very difficult for many reasons. For instance, the resulting perturbation to the vertical temperature gradient will affect temperatures at other depths within the lithosphere, which will in turn affect densities and amounts of isostatic subsidence. This simple treatment gives first-order approximate solutions, to illustrate the underlying physics and quantify the main differences compared with conventional solutions.

Suppose that during extension thickness $E$ of lower crust is lost by channel flow to outside the extensional province. After extension by factor $\beta$ what is left has thickness $(T_c/\beta - E)$. Lithosphere thickness is now $(S_s + T/\beta - E + T_a)$, and its weight is proportional to $[S_s\,\rho_i + T_c\,\rho_c/\beta - E\rho_c + (T - T_c)\,\rho_m/\beta + T_a\,\rho_a]$. Thus

$$T = S_s + T/\beta - E + T_a \quad \text{(A1.8)}$$

and

$$T_c\rho_c + (T - T_c)\rho_m = S_s\rho_i + T_c\rho_c/\beta - E\rho_c + (T - T_c)\rho_m/\beta + T_a\rho_a \quad \text{(A1.9)}$$

so

$$S_s = (1 - 1/\beta)\frac{T_c(\rho_m - \rho_c) - T(\rho_m - \rho_a)}{\rho_a - \rho_i} + E\frac{\rho_a - \rho_c}{\rho_a - \rho_i}. \quad \text{(A1.10)}$$

Because $\rho_a > \rho_c$ and $\rho_a > \rho_i$, for a given $\beta$ this predicted subsidence exceeds the amount from (A1.3).

Let $E_f$ denote the total crustal thickness lost. After thermal equilibrium is restored, the final lithosphere thickness is $(S_f + T_c/\beta - E_f + T_m)$, and its weight is proportional to $(S_f\,\rho_i + T_c\,\rho_c/\beta - E_f\,\rho_c + T_m\,\rho_m)$. Thus

$$T = S_f + T_c/\beta - E_f + T_m \quad \text{(A1.11)}$$

and

$$T_c\rho_c + (T - T_c)\rho_m = S_f\rho_i + T_c\rho_c/\beta - E_f\rho_c + T_m\rho_m \quad \text{(A1.12)}$$

so

$$S_f = (1 - 1/\beta)\frac{T_c(\rho_m - \rho_c)}{\rho_m - \rho_i} + E_f\frac{\rho_m - \rho_c}{\rho_m - \rho_i} \quad \text{(A1.13)}$$

which can be compared with (A1.6). As before, the second term on the right-hand side is positive, indicating that failure to allow for loss of crustal material will overestimate the $\beta$ value responsible for a given amount of subsidence and sedimentation.

If outward channel flow isostatically compensates all sedimentation, then

$$E_f\rho_c = S_f\rho_i \quad \text{(A1.14)}$$

and (A1.13) gives

$$S_f = (1 - 1/\beta)\frac{T_c\rho_c(\rho_m - \rho_c)}{\rho_m(\rho_c - \rho_i)} \quad \text{(A1.15)}$$

which can also be compared with (A1.6).

*Discussion*

Comparing (A1.6) and (A1.15) indicates that failure to allow for outward lower-crustal channel flow causes subsidence for any $\beta$ to be underestimated by a factor $R_f$ where

$$R_f = \frac{(1 - \rho_i/\rho_m)}{(1 - \rho_i/\rho_c)}. \quad \text{(A1.16)}$$

With $\rho_a = 3100$ kg m$^{-3}$, $\rho_c = 2700$ kg m$^{-3}$ and $\rho_m = 3200$ kg m$^{-3}$, $R_f$ is thus 1.45 for $\rho_i = 2000$ kg m$^{-3}$, 1.69 for $\rho_i = 2200$ kg m$^{-3}$, 2.25 for $\rho_i = 2400$ kg m$^{-3}$ and 5.06 for $\rho_i = 2600$ kg m$^{-3}$. These values span thin, unconsolidated sediment to ancient, compacted and well-lithified sediment. Failure to account for outward flow can thus cause dramatic underestimation of basin subsidence.

An estimate for long-term subsidence-derived extension factor $\beta_s$ can be derived from (A1.15) by equating the observed sediment thickness $T_s$ to the predicted value of $S_f$:

$$\beta_s/(\beta_s - 1) = \frac{T_c\rho_c(\rho_m - \rho_c)}{T_s\rho_m(\rho_c - \rho_i)}. \quad \text{(A1.17)}$$

This only approximates the real situation, because some outward flow will isostatically compensate mantle upwelling and some sedimentation will occur without outward flow. The crustal thickness lost, $E_f$, will equal

$$E_f = T_c/\beta - T_b, \quad \text{(A1.18)}$$

where $T_b$ is the final thickness of crustal basement. Substituting (A1.18) into (A1.15) makes all $\beta$-dependent terms cancel. Equating $T_s$ to $S_f$, as before, now gives:

$$T_c = T_s\frac{\rho_m - \rho_i}{\rho_m - \rho_c} + T_b. \quad \text{(A1.19)}$$

This means that the original crustal thickness can be estimated from $T_s$ and $T_b$.

The extension factor $\beta_w$ derived from the overall loss of weight of a crustal column can be estimated as the ratio of initial to final weights, proportional to $\rho_c\,T_c$, and $(T_s\,\rho_i + T_b\,\rho_c)$:

$$\beta_w = \frac{\rho_c T_c}{T_s\rho_i + T_b\rho_c}. \quad \text{(A1.20)}$$

This also correctly estimates extension if all sedimentation has isostatically compensated outward flow.

Finally, after thermal equilibrium is restored, the true extension factor $\beta_t$ (assuming all sedimentation is isostatically compensated by lower-crustal flow) can be estimated when conventional modelling gives extension factor $\beta_o$ instead. Combining (A1.6) and (A1.15) using $R_f$ in (A1.16) gives:

$$\beta_t = \frac{\beta_o R_f}{1 + \beta_o(R_f - 1)}. \quad \text{(A1.21)}$$

## APPENDIX 2
## CONDITIONS FOR OUTWARD LOWER-CRUSTAL CHANNEL FLOW BENEATH AN EXTENSIONAL BASIN

The pre-requisite for outward lower-crustal channel flow from beneath an extensional basin is a positive lithostatic pressure anomaly $\delta P$, such that lithostatic pressure at the base of the brittle layer is greater beneath the basin than beneath the sink of flow. At first sight this condition seems unlikely to be satisfied, because extension will thin the brittle layer beneath the basin, reducing lithostatic pressure at its base. However, sedimentation will raise the lithostatic pressure at the base of the brittle layer, and erosion of the surroundings of the basin will reduce the lithostatic pressure at the base of the brittle layer there. Both these processes can thus adjust conditions in favour of outward channel flow.

Suppose no erosion occurs in the surroundings to a basin, which

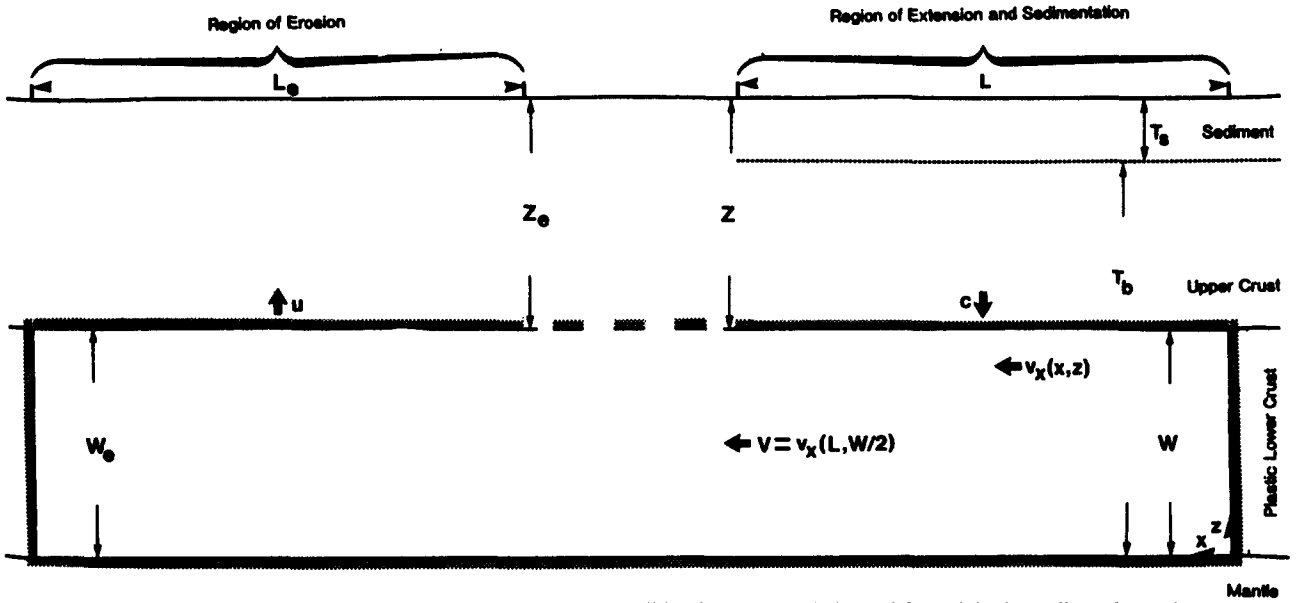


Fig. A1. Schematic diagram summarizing parameters describing lower-crustal channel flow. Stipple outlines the region where this flow is assumed to occur.

extends by factor $\beta$ whilst sediment thickness $T_s$ is deposited. Let $T_0$ denote the initial thickness of the brittle layer. Initial lithostatic pressure at the base of the brittle layer beneath both the basin and its surroundings is $\rho_c\, g\, T_0$. Neglecting effects of thermal conduction (i.e. regarding extension as instantaneous), after extension the lithostatic pressure at the base of the brittle layer is $(\rho_c\, g\, T_0/\beta + \rho_s\, g\, T_s)$. The condition for outward channel flow $\delta P > 0$ is thus:

$$\rho_c g T_0/\beta + \rho_s g T_s > \rho_c g T_0 \qquad \text{(A2.1)}$$

or

$$T_s > \frac{\rho_c T_0(\beta - 1)}{\rho_s \beta}. \qquad \text{(A2.2)}$$

Erosion of a basin's surroundings can reduce the sediment thickness required to drive outward channel flow. For instance, if the initial dimensions of a basin and its eroding surroundings are the same, and all basin sediment is derived from these surroundings, the condition for outward flow becomes

$$T_s > \frac{\rho_c T_0(\beta - 1)}{\rho_s \beta(\beta + 1)}. \qquad \text{(A2.3)}$$

## APPENDIX 3
## DYNAMICS OF LOWER-CRUSTAL CHANNEL FLOW

This Appendix addresses the dynamics of outward lower-crustal channel flow for a region that is neither extending nor shortening, but which is experiencing sedimentation and whose surroundings are eroding. This first-order treatment assumes that lower-crustal channel flow is isoviscous laminar flow between parallel horizontal boundaries at vertical positions z = 0 and z = W (Fig. A1), which is driven by a horizontal pressure gradient, $dP/dx$. Such flow has a parabolic profile of horizontal velocity $v_x(z)$, of the form

$$v_x(x,z) = \frac{1}{2\eta}\frac{dP(x)}{dx}(z^2 - Wz) \qquad \text{(A3.1)}$$

(e.g. Turcotte & Schubert 1982, p. 234), with $dP/dx$ negative in the direction of flow. I assume that the boundaries to the flow converge at rate $c$ across length $L$ in the $x$-direction, from $x = 0$ to $x = L$. Because the volume flux passing through each element of the lower-crustal channel is required to be proportional to $x$, I assume that $dP/dx$ is proportional to $x$, such that (A3.1) can be written as

$$v_x(x,z) = A(x)(zW - z^2) \qquad \text{(A3.2)}$$

with $A$ proportional to $x$. Total volume flux $Q$ (per unit length in the along-strike $y$-direction) is thus $L\,c$. By integrating $v_x$ over $z = 0$ to $W$ at $x = L$, and equating the resulting horizontal volume flux to the convergent volume flux of the channel boundaries, $A(L)$ can be determined to be $6\,c\,L/W^3$, such that

$$v_x(x,z) = \frac{6cx(zW - z^2)}{W^3}. \qquad \text{(A3.3)}$$

From (A3.1), $dP/dx$ is thus required to satisfy

$$\frac{dP}{dx} = \frac{12c\eta x}{W^3}. \qquad \text{(A3.4)}$$

The maximum horizontal velocity at each $x$ occurs at $z = W/2$, and is

$$v_x(x,W/2) = \frac{3cx}{2W}. \qquad \text{(A3.5)}$$

The horizontal velocity gradient at the boundaries of the channel is thus

$$\frac{dv_x(x,z=0,W)}{dz} = \pm\frac{6cx}{W^2}. \qquad \text{(A3.6)}$$

The viscous force per unit area on each boundary of the channel will thus be $\eta\, dv_x/dz$, where $\eta$ is the viscosity of material in the channel. The total viscous force $F_x$ acting per unit along-strike length on each boundary of the channel is obtained by integration over the range $x = 0$ to $L$, and is

$$F_x = \frac{3\eta c L^2}{W^2}. \qquad \text{(A3.7)}$$

For any sedimentary basin that is isostatically compensated by outward lower-crustal flow, the parameter $c$ will approximately equal the sedimentation rate, for which I adopt the value 0.1 mm year$^{-1}$. For a basin with width $L$ ~300 km and thickness $W$ of the plastic lower crust ~10 km, $F_x$ for each boundary of the lower-crustal channel is $\sim 10^{10}$ N m$^{-1}$ for $\eta \sim 10^{18}$ Pa s or $\sim 10^{11}$ N m$^{-1}$ for $\eta \sim 10^{19}$ Pa s. Numerical modelling (e.g. Kusznir & Park 1987, Kusznir 1991), establishes that the strong parts of the continental lithosphere, the upper crust and mantle parts, can withstand horizontal forces of the order of $\sim 10^{12}$ N m$^{-1}$. Consequently, it is feasible for such flow to occur in the lower crust, without affecting the rest of the lithosphere, provided the lower crust has viscosity $< \sim 10^{20}$ Pa s. Many analyses support lower-crustal viscosity smaller than this. For example, Reilinger (1986) determined lower-crustal viscosity as $\sim 10^{19}$ Pa s by modelling viscoelastic relaxation following a large normal-faulting earthquake. Kruse *et al.* (1991) showed that the effective viscosity (the ratio of stress to strain rate) of material in a lower-crustal channel is likely to be no greater than $\sim 10^{19}$ Pa s under a wide range of conditions.

Although viscous forces acting on the boundaries to the channel are

expected to be too small to break the lithosphere, the reaction to them acting on the channel material will oppose the force caused by any lithostatic pressure anomaly, which drives the channel flow. Suppose the excess lithostatic pressure at the base of the brittle layer beneath the basin is $\delta P$. This can be related to the equivalent excess thickness of crustal basement $\delta Z$, where

$$\delta P = \rho_c \mathbf{g} \delta Z. \tag{A3.8}$$

If the channel thickness is $W$ beneath both the basin and the sink of flow, the net force (per unit along-strike length) driving this flow will thus be

$$F_p = \rho_c \mathbf{g} \delta Z W. \tag{A3.9}$$

The equation of equilibrium of the material undergoing such flow will thus have $F_p$ equal to the total viscous force (per unit along-strike length) opposing this flow. Beneath the source of the flow, each boundary of the channel will contribute a force equal to $F_x$ in (A3.7). Assuming that the channel has the same width $W$ and length $L$ beneath the sink, each boundary there will also make the same contribution. The total viscous force opposing channel flow is thus $4 F_x$. Substituting for $c$ from (A3.5) using $V = v_x(L, W/2)$ gives

$$F_x = \frac{4\eta L V}{W} \tag{A3.10}$$

so

$$\delta Z = \frac{16\eta L V}{W^2 \mathbf{g} \rho_c} = \frac{12\eta c L^2}{W^3 \mathbf{g} \rho_c}. \tag{A3.11}$$

Equation (A3.11) can also be expressed in terms of $\delta P$, which equals $\rho_c$ $\mathbf{g}$ $\delta Z$.

An alternative way to obtain these results for $F_x$ and $\delta Z$ is as follows. Assuming the channel maintains uniform width $W$, the force required to drive flow from between $x = 0$ and $L$ can be obtained as $W$ times the integral of $dP/dx$ across this range of $x$, and is

$$F_r = \frac{6\eta c L^2}{W^2}. \tag{A3.12}$$

$F_r$ is thus double $F_x$ from (A3.10). Because an equal force is required to drive the flow into the sink, the total driving force is thus $4 F_x$, as before. From similar integration, the pressure change required between $x = 0$ and $L$ is $6 \eta c L^2/W^3$. Doubling this to account for the contribution of the sink, and equating the result with $\rho_c$ $\mathbf{g}$ $\delta Z$ provides an alternative method for obtaining (A3.11).

The above equations can be rearranged in terms of $Q$ rather than $c$. For instance, (A3.11) becomes:

$$Q = cL = uL_e = \frac{\delta Z W^3 \mathbf{g} \rho_c}{12\eta L}. \tag{A3.13}$$

## APPENDIX 4
## EFFICIENCY OF LOWER-CRUSTAL CHANNEL FLOW

The cyclic process described in Fig. 4 is driven by the gravitational potential energy released as material subsides within a sedimentary basin. This does work against viscous forces in the lower crust, and against gravity to uplift upper-crustal material beneath the source region of the sediment. Let $W_1$ denote the rate at which energy is released by subsidence within the basin, $W_2$ denote the rate of work done against gravity uplifting the sediment source region, and $W_3$ and $W_4$ denote the rates of work done against viscous forces in the lower crust, beneath the basin and beneath the sediment source region. Throughout this analysis. Neglecting other processes, from conservation of energy,

$$W_1 = W_2 + W_3 + W_4. \tag{A4.1}$$

One may liken this cycle to the operation of a machine, with $W_1$ the energy input, $W_2$ the useful work output, and $W_3 + W_4$ energy 'wasted' by 'mechanical losses'. From the usual definition of efficiency, $\Phi$,

$$\Phi = \frac{W_2}{W_1} \tag{A4.2}$$

or, from (A4.1),

$$\Phi = \frac{W_2}{W_2 + W_3 + W_4}. \tag{A4.3}$$

In hydraulic machinery, the fluid that couples the input and output has low viscosity, so energy losses in it are small; efficiency is nearly 1 (or 100%). It is interesting to address whether this is also true for energy released or absorbed by tectonic elevation changes that are coupled via viscous flow in the lower-crust.

$L$, $L_e$, $Z_e$, $\rho_c$, $\delta Z$, $\mathbf{g}$, $c$, $u$ and $t$, were defined in Appendix 3. Let $J$ and $J_e$ denote the along-strike lengths of sedimentation and erosion, and let $U$ and $E$ denote the thicknesses of material lost by erosion and channel flow, with $U = u t$ and $E = c t$. With lithostatic pressure at the base of the brittle layer given by $\rho_c$ $\mathbf{g}$ $Z_e$ beneath the sink of channel flow and $\rho$ $\mathbf{g}$ $(Z_e + \delta Z)$ beneath the source, $W_1$ and $W_2$ can be estimated as

$$W_1 = \rho_c \mathbf{g} (Z_e + \delta Z) LJE \tag{A4.4}$$

and

$$W_2 = \rho_c \mathbf{g} Z_e L_e J_e U. \tag{A4.5}$$

To estimate $W_3$, consider an element with length $dx$, width $J$ and thickness $dz$, in the upper half of the lower-crustal channel where horizontal velocity $v_x(x,z)$ increases with depth. The viscous forces acting its top and base are $[-\eta\, dv_x(x,z)/dz\, dx]$ and $[\eta\, dv_x(x,z + dz)/dz\, dx]$. The net viscous force $dF$ acting on it is thus

$$dF = \eta J \frac{d^2 v_x(x,z)}{dz^2} dx\, dz. \tag{A4.6}$$

The work done on the element by viscous forces in time $t$, $dW$, equals $dF$ times the distance it moves, which is $v_x t$. Using (A3.3) for $v_x$ beneath the basin,

$$\frac{d^2 v_x(x,z)}{dz^2} = \frac{-12cx}{W^3} \tag{A4.7}$$

so

$$dW = \frac{12cJ\eta t}{W^3} x v_x\, dx\, dz. \tag{A4.8}$$

Allowing for an equal contribution from the lower half of the channel, $W_3$ is double the integral of $dW$ over $x = 0$ to $L$ and $z = 0$ to $W/2$. Substituting from (A3.3), it is

$$W_3 = \frac{4c^2 J \eta L^3 t}{W^3}. \tag{A4.9}$$

$W_4$ is given by a similar equation, with $u$, $J_e$, $L_e$ and $W_e$ replacing $c$, $J$, $L$ and $W$.

The simplest case is symmetric channel flow, where $c = u$, $W = W_e$, $J = J_e$, and $L = L_e$, so $W_3 = W_4$, thus,

$$\Phi = \frac{\rho_c \mathbf{g} Z_e L_e U}{\rho_c \mathbf{g} Z_e L_e U + 8u^2 \eta L_e^3 t / W_e^3} = \frac{1}{1 + 8u\eta L_e^2/(\rho_c \mathbf{g} Z_e W_e^3)} \tag{A4.10}$$

since $U = u t$. If $\phi$ is expressed as $1/(1 + k)$, then using (A3.13)

$$k = \frac{8u\eta L_e^2}{\rho_c \mathbf{g} Z_e W_e^3} = \frac{8Q\eta L_e}{\rho_c \mathbf{g} Z_e W_e^3}. \tag{A4.11}$$

With $u = 0.1$ mm year$^{-1}$ and $L_e = 300$ km, $Q$ is $3 \times 10^{-5}$ km$^3$ year$^{-1}$ per km of along-strike length. With $\eta = 10^{19}$ Pa s, $\rho_c = 2700$ kg m$^{-3}$, $\mathbf{g}$ = 10 m s$^{-2}$, $Z_e = 10$ km and $W_e = 10$ km, then $k$ is $\sim 10^{-1}$ and $\phi$ is nearly 1.